Data-driven real-time predictive control for industrial heating loads

Chuanshen Wu, Yue Zhou [*], Jianzhong Wu

School of Engineering, Cardiff University, Cardiff, UK

ARTICLE INFO

ABSTRACT

Uncertainties and computational complexity are two growing challenges in scheduling industrial heating loads. In this paper, a data-driven real-time predictive control approach is proposed to deal with these challenges in the industrial scheduling of bitumen tanks. Specifically, predictive control technology is utilized to leverage the updated information to mitigate the negative impact of past uncertainties in equipment parameters and external environmental factors, which may lead to temperature constraint violations in the bitumen tank operation processes. Meanwhile, a data-driven method using artificial neural networks (ANN) is developed to ensure efficient computation for real-time predictive control. Moreover, a two-layer control method is devised to reduce the calculation time for day-ahead optimal scheduling of a large scale of bitumen tanks, aiming to generate sufficient high-quality data for training ANN. In the two-layer control method, the clustered temperature transfer processes of bitumen tanks are analyzed and modeled for the first time. Simulation results indicate that the two-layer control method can significantly reduce the computational time required for the day-ahead optimal scheduling of bitumen tanks, facilitating the generation of a large amount of high-quality data for training ANN. Subsequently, the application of ANN enables real-time predictive control, helping to eliminate the negative impact of uncertainties.

1. Introduction

The exploration of flexibility within industrial production processes is a prominent research area in the industrial sector [1]. This field is dedicated to investigating innovative strategies that harness the inherent flexibility of industrial production processes to optimize electricity consumption without impacting normal production or services provision [2].

In real-world scenarios, numerous uncertainties exist in industrial production processes, such as those related to renewable energy generation [3], real-time electricity prices [4], and electrical load demand [5]. These uncertainties may cause deviations between the actual and expected states of the industrial processes, resulting in poor control performance. For industrial heating loads, the temperature transfer processes are susceptible to uncertainties in equipment parameters and environmental factors, in addition to the aforementioned uncertainties, which are generally neglected in previous research. For example, the heat dissipation rate of industrial heating loads changes with variations in external temperature, which may potentially result in temperature constraint violations during their operational processes.

In this paper, real-time predictive control technology [6] is utilized

to address the issues caused by uncertainties in equipment parameters and environmental factors in the control of industrial heating loads. During the real-time predictive control process, the current states and forecasting values in the control model of industrial heating loads can be updated based on real-time feedback, which is important to mitigate the negative impact of the previous uncertain factors [7].

Real-time predictive control requires high computational efficiency to ensure that it can be implemented at every time step. However, in industrial sites, providing balancing and network services to the main grid require coordinating various flexibility sources and thus involve a global optimization, which is usually formulated as a mixed integer programming (MIP) problem [8]. This is an NP-hard (non-deterministic polynomial-time hard) problem with high computational complexity, making it challenging to conduct real-time predictive control. At present, there are several main categories of approaches for solving NP-hard problems, such as exact methods and heuristic algorithms. Exact methods aim to find an optimal solution by exploring the entire search space, which guarantee the global optimum, but they can be computationally expensive for large-scale problems [9]. Heuristic algorithms are designed to find suitable solutions quickly, but they may not guarantee to find the global optimum and can get stuck in local optima [10].

Moreover, integer programming solvers, such as CPLEX, are specialized software packages to solve MIP problems, which have been widely used in industry and academia [11]. However, as the scale of the problem and the number of integer variables increases, the solution efficiency of all the above approaches in real-time predictive control may become a bottleneck.

Nowadays, data-driven methods, such as artificial neural networks (ANN) [12], deep neural networks (DNN) [13], and deep reinforcement learning (DRL) [14], have opened up the possibility for real-time predictive control in complex industrial processes. These powerful machine learning algorithms can learn and model complex, nonlinear relationships between input and output data [15]. Compared to DNN and DRL, which are typically applied in complex tasks [16], the implementation and training of ANN are more easily manageable and better suited for this study. The utilization of ANN can significantly reduce the computational burden as it can quickly process input data and generate control commands as output data without intricate calculations [17]. Basically, the effectiveness of ANN depends on the quality and quantity of historical data used to train it. As asserted in [18], ensuring that the training data possesses both good quality and a sufficiently large quantity is crucial for the ANN to learn complex input-output relationships. However, historical industrial operation or scheduling data are typically based on experience and automatic control, which may not represent the optimal operation. For example, in the historical operation involving industrial heating loads, the most commonly employed method is through an automatic temperature control mechanism, while overlooking the optimal adjustment of the switch status through manual control [19]. Therefore, it is necessary to develop an efficient control method for industrial heating loads that can effectively deal with large-scale NP-hard problems, facilitating the generation of a substantial amount of high-quality data (at least thousands of samples [20]) for training ANN.

Two-layer control is a concept of hierarchical architecture designed to address complex control problems where a large number of control variables need to be considered [21]. The key advantages of the two-layer control architecture are its ability to significantly reduce computational time and ensure that computational time is not influenced by the increasing scale of control objects. In specific, the role of the upper layer is to reduce the complexity of the control problem by clustering control objects together. The lower layer focuses on optimizing the control of each individual object based on the results obtained from the upper-layer clustering control. In the existing studies, the authors in [22] proposed a two-layer frequency control framework for large-scale distributed energy storages that can be separated into several energy storage clusters to solve the heavy computational burden. A two-layer optimization framework was established in [6] to speed up the calculation efficiency of energy management of a large scale of electric vehicles. The authors in [23] implemented a two-layer demand response program to reduce the total power consumption of household appliances during peak hours by clustering the different operation modes of household appliances. However, as far as the authors know, there has been no research focusing on the two-layer control of industrial heat loads for speeding up scheduling purposes. This is because, compared to loads such as electric vehicles, energy storages, and household appliances, industrial heat loads exhibit more complex clustering characteristics. For example, the temperature transfer inside each industrial heat load is nonlinear. This arises from the fact that, when the internal temperature of the industrial heat load is high, the large temperature difference with the external environment results in a higher rate of heat dissipation; whereas at lower internal temperatures, the heat dissipation rate is lower [24]. Therefore, analyzing the clustered temperature transfer characteristics of industrial heat loads is challenging. Meanwhile, due to various factors such as different initial temperatures and uncertainties, the temperature distribution within the population of industrial heat loads is discrete [25], making it challenging to set the limits for the average temperature of industrial heat loads during the
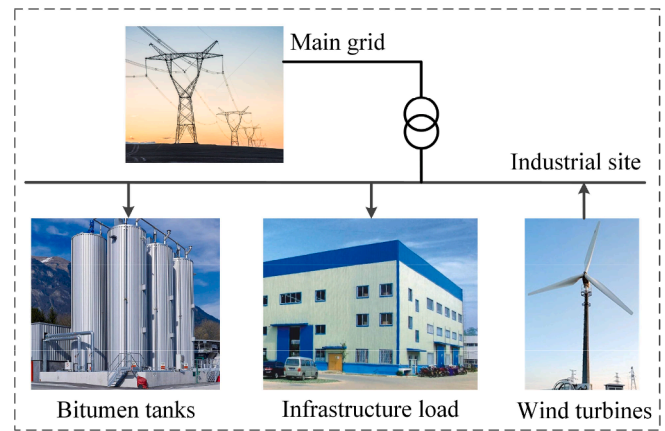
clustering temperature transfer processes.

Based on the above analysis, ANN-based real-time predictive control is an effective approach to address the computational complexity and uncertainty issues in the control processes of industrial heating loads. Moreover, a prerequisite for this approach is to develop an efficient control method that can generate sufficient high-quality training data for the ANN. In this paper, an industrial site with a large scale of bitumen tanks is analyzed as a representative of industrial heating loads. The main contributions of this work are as follows.

1) A two-layer control method is proposed to deal with the calculation complexity of day-ahead control of a large scale of bitumen tanks. The upper-layer cluster control optimizes the total number of bitumen tanks to be switched ON at each time slot, while the lower-layer model distributes the obtained number of switching ON within the bitumen tank population.
2) In the proposed two-layer control model, the clustered temperature transfer processes of bitumen tanks are analyzed and modeled for the first time, for the purpose of expediting scheduling. Meanwhile, the limits for the average temperature of bitumen tanks are well defined by considering the clustered temperature transfer characteristics.
3) An ANN-based real-time predictive control method is developed based on the sufficient training data obtained from the proposed two-layer control method, aiming to further speed up the solution efficiency and mitigate the negative impact of uncertainties in equipment parameters and environmental factors during the operational processes of bitumen tanks.

The paper is organized as follows. Section 2 presents the control mechanism of industrial bitumen tanks. Section 3 formulates the two-layer control method of bitumen tanks. Section 4 analyzes the uncertainties in the operation of bitumen tanks and develops the ANN-based real-time predictive control approach. Section 5 presents the results of case studies. Finally, the conclusions and future directions are presented in Section 6.

2. Control mechanism of bitumen tanks

2.1. Industrial sites with bitumen tanks

Fig. 1 shows that the main power elements in an industrial site include bitumen tanks, infrastructure load, and on-site wind turbines. The infrastructure load refers to the amount of power required by the industrial site to operate its essential functions consistently throughout the day.

Generally, a bitumen tank is equipped with an electric heater to control the heating to in-tank temperature within a certain range,
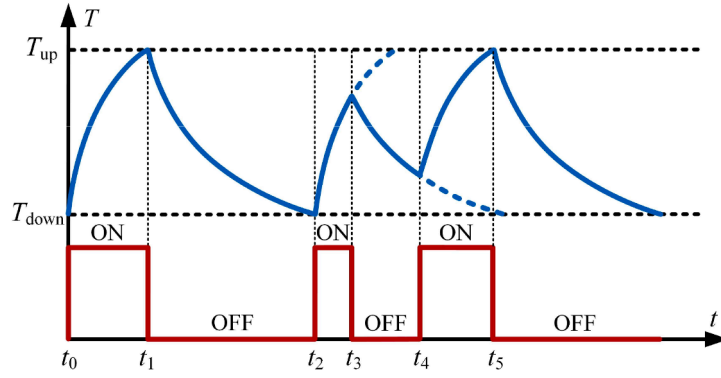

Fig. 1. An industrial site of bitumen tanks.

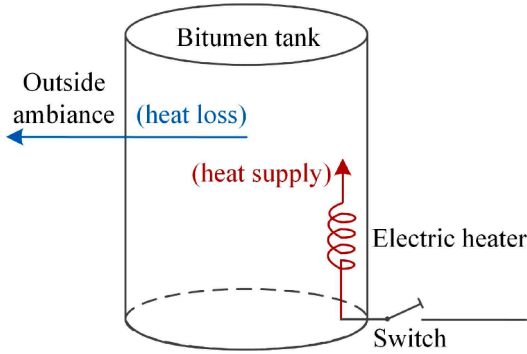**Fig. 2.** The temperature control mechanism of a bitumen tank.

Fig. 3. The heating transfer process of a bitumen tank.

typically between 150 °C and 180 °C, ensuring the fluidity and viscosity of the stored bitumen so that it can be used when needed [26]. Meanwhile, bitumen tanks have to consume a large amount of energy to maintain the temperature [19]. As clean and low-cost renewable energy, on-site wind power can provide a significant amount of electricity to bitumen tanks and reduce the energy demand of the industrial site from the main grid [27]. Therefore, it is necessary to manage the operation of bitumen tanks to promote the absorption of on-site wind power and improve the characteristics of the power demand curve of the industrial site for the benefits of the main power grid.

2.2. Temperature control mechanism

The bitumen tank has two temperature control processes, namely heating, and cooling. When the switch of the electric heater is turned ON, the temperature of bitumen increases. On the contrary, when the switch is turned OFF, the temperature of bitumen naturally cools down.

As shown in Fig. 2, there are typically two ways to adjust the switch status of the electric heater of the bitumen tank. The first way is through an automatic temperature control mechanism [19]. This mechanism is designed to maintain the temperature of the bitumen within a specific range by automatically turning the switch ON and OFF as needed. When the temperature of a bitumen tank reaches the upper limit (e.g., $t_{1/5}$ in Fig. 2), the mechanism turns OFF its switch to prevent overheating. By contrast, when the temperature falls below the lower limit (e.g., t_2 in Fig. 2), the mechanism turns ON its switch to raise the temperature. The second way to adjust the switch status is through manual control. In this case, the system can manually turn the switch ON or OFF at any time (e. g., $t_{3/4}$ in Fig. 2), regardless of the current temperature of the bitumen tank. This method provides more flexibility and allows for adjustments based on the specific needs of the operation.

Fig. 3 depicts the heating transfer process of a bitumen tank. The corresponding mathematical expressions for the heating transfer process

are introduced below:

$$P_{supply} = P_{rate} \times x \tag{1}$$

$$P_{loss} = U \times A \times (T - T_{amb}) \tag{2}$$

$$P_{net} = P_{supply} - P_{loss} \tag{3}$$

$$P_{net} = c_v \times m \times \frac{dT}{dt} \tag{4}$$

$$\frac{dT}{dt} = \frac{P_{rate} \times x - U \times A \times (T - T_{amb})}{c_v \times m} \tag{5}$$

where P_{supply} is the heat supply rate; P_{rate} is the rated power of heating; x is the switch state, with 1 indicating the electric heater is turned ON and 0 indicating the electric heater is turned OFF; P_{loss} is the heat loss rate; U is the overall heat transfer coefficient; A is the area of bitumen tank; T is the temperature of bitumen; T_{amb} is the temperature of outside ambiance; P_{net} is the net rate of heat transfer; c_v is the heat capacity of the bitumen; m is the mass of bitumen.

Eqs. (1) and (2) provide the heat supply rate and heat loss rate for each bitumen tank. Eq. (3) represents the net rate of heat transfer, leading to a change in temperature inside the bitumen tank. Eq. (4) illustrates the relationship between the net rate of heat transfer and the rate of internal temperature change. Finally, Eq. (5) determines the rate of internal temperature change for the bitumen tank under different switch states.

By controlling the switch state x of each electric heater, the power consumption characteristics of bitumen tanks in the industrial site can be optimized while maintaining the desired temperature range of bitumen.

3. Two-layer control method of bitumen tanks

3.1. Direct control method

The direct control objective of bitumen tanks in an industrial site is to minimize the peak-to-valley difference of the demand power curve from the main grid while considering the absorption of onsite wind power, which is given as follows:

$$\min f = \max_{1 \le h \le H} \left(\sum_{i=1}^{N} x_{i,h} \times P_{rate} - C_h \right) - \min_{1 \le h \le H} \left(\sum_{i=1}^{N} x_{i,h} \times P_{rate} - C_h \right) \tag{6}$$

$$s.t. T_{i,h} = T_{i,h-1} + \frac{P_{rate} \times x_{i,h} - U \times A \times (T_{i,h-1} - T_{amb}^h)}{c_v \times m} \times \Delta t, \forall i, \forall h \tag{7}$$

$$T_{down} \le T_{i,h} \le T_{up}, \forall i, \forall h \tag{8}$$

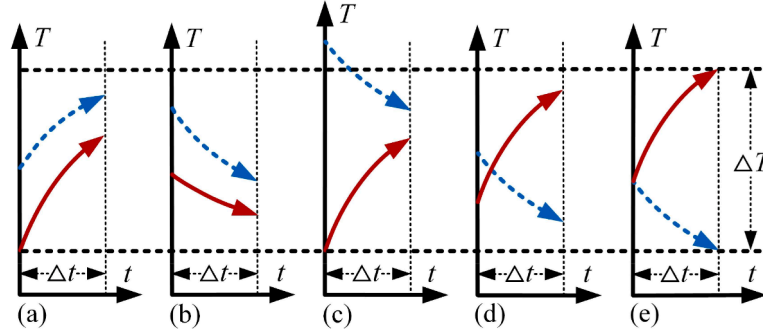where H is the length of the time horizon; N is the number of bitumen

Fig. 4. The temperature evolution process of the two bitumen tanks.

tanks; $x_{i,h} \in \{0, 1\}$ is the switch state of the ith electric heater at hth time slot; C_h is the value of wind power output minus infrastructure load at hth time slot; $T_{i,h}$ is the temperature of ith bitumen tank at hth time slot; Δt is the length of each time slot; T_{amb}^h is the temperature of outside ambiance at hth time slot. $T_{up/down}$ is the upper/lower temperature limit of bitumen tanks.

Eq. (7) gives the temperature transfer process of each bitumen tank. Eq. (8) expresses the upper/lower limit of the temperature of each bitumen tank.

The direct control of bitumen tanks is formulated as an integer programming (IP) problem, which is known to be NP-hard. As the number of bitumen tanks and the length of time horizon increases, the computational complexity of finding an optimal solution to the day-ahead control of bitumen tanks increases exponentially.

3.2. Two-layer control method

To address the above-mentioned computational burden, this subsection proposes a two-layer control method. The upper-layer clustered control decides the total number of bitumen tanks that should be turned ON at each time slot. The lower-layer distributes the total number of switches that should be opened to each bitumen tank at each time slot.

1) Upper-layer clustered control

Same as the direct control method, the objective of the upper-layer clustered control is to minimize the peak-to-valley difference of the demand curve:

$$\min f = \max_{1 \le h \le H}(x_h \times P_{rate} - C_h) - \min_{1 \le h \le H}(x_h \times P_{rate} - C_h) \tag{9}$$

where $0 \le x_h \le N$ is the number of bitumen tanks to be turned ON at the hth time slot.

According to (7), the temperature transfer constraints of each bitumen tank in the industrial site are listed as:

$$\begin{cases} T_{1,h} = T_{1,h-1} + \dfrac{P_{rate} \times x_{1,h} - U \times A \times (T_{1,h-1} - T_{amb}^h)}{c_v \times m} \times \Delta t \\ T_{2,h} = T_{2,h-1} + \dfrac{P_{rate} \times x_{2,h} - U \times A \times (T_{2,h-1} - T_{amb}^h)}{c_v \times m} \times \Delta t \\ \dots \\ T_{N,h} = T_{N,h-1} + \dfrac{P_{rate} \times x_{N,h} - U \times A \times (T_{N,h-1} - T_{amb}^h)}{c_v \times m} \times \Delta t \end{cases} \tag{10}$$

By summing all the formulas in (10) and taking the average, the clustered temperature transfer constraint of bitumen tanks can be obtained as follows:

$$\overline{T}_h = \overline{T}_{h-1} + \frac{P_{rat} \times \frac{x_h}{N} - U \times A \times (\overline{T}_{h-1} - T_{amb}^h)}{c_v \times m} \times \Delta t \tag{11}$$

where $\overline{T}_h$ is the average temperature of bitumen tanks at the hth time slot.

To ensure compliance with the temperature constraints for each individual bitumen tank, it is crucial to maintain a certain gap between the average temperature of all the bitumen tanks and the limits (T_{up} and T_{down}). This is necessary because the temperatures of the bitumen tanks are distributed discretely around the average temperature. Therefore, the lower/upper limit of the average temperature of bitumen tanks is given as follows:

$$T_{down} + \Delta T \le \overline{T}_h \le T_{up} - \Delta T, \forall h \tag{12}$$

where ΔT is the magnitude of the gap, and the specific value is analyzed and provided in the next subsection.

In the direct control method, the size of control variables is $N \times H$, while in the upper-layer clustered control, the size is reduced and remains at $1 \times H$, making it possible to control a large number of bitumen tanks efficiently.

2) Lower-layer state distribution

After obtaining the total number of bitumen tanks that should be ON (i.e., $\{x_h\}_{h=1}^H$) through the upper-layer clustered control, it is necessary to make further decision regarding which specific bitumen tanks should be ON (i.e., the state distribution). The principle of lower-layer state distribution is to prioritize turning ON the switches of bitumen tanks with lower temperatures at each time slot. This principle keeps the temperatures of the bitumen tanks away from the upper and lower limits as much as possible, thus preventing temperature constraint violations.

3.3. Magnitude of the gap

According to the lower-layer state distribution principle introduced in Section 3-2-2), at any specific time slot, two arbitrary bitumen tanks within a population of bitumen tanks can have three different combinations of the ON/OFF states. In Case 1, both bitumen tanks are turned ON. In Case 2, both bitumen tanks are turned OFF. In Case 3, the bitumen tank with lower temperature is turned ON while the bitumen tank with higher temperature is turned OFF.

Next, to obtain the magnitude of the gap (i.e., the value of ΔT) mentioned in (12), the following lemma is introduced. *Lemma A*: For a population of bitumen tanks controlled by the two-layer optimal scheduling model, if $\delta_h \le \Delta T$ at the time step h, then for the next time step there must be $\delta_{h+1} \le \Delta T$, where δ is the width of the temperature distribution of the bitumen tank population and equals to the difference between the maximum and minimum temperature in the population.

The proof of *Lemma A* is given as follows. According to (7), in Case 1, when both bitumen tanks are turned ON, the bitumen tank with a lower temperature heats up faster (as depicted in Fig. 4(a)). In Case 2, when both bitumen tanks are turned OFF, the bitumen tank with a higher temperature cools down faster (as depicted in Fig. 4(b)). Therefore, the
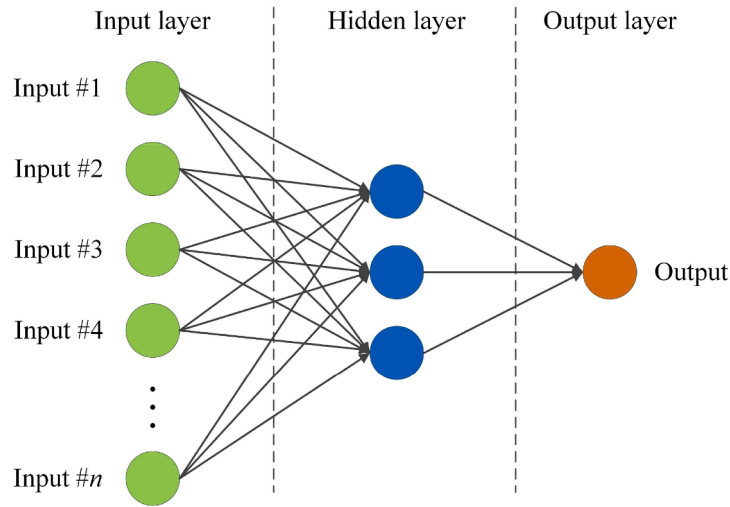
Fig. 5. Schematic diagram of an ANN.

temperature difference between the two bitumen tanks in both Cases 1 and 2 will decrease throughout the entire Δt period. According to the initial temperature difference between the two bitumen tanks, Case 3 can be divided into two scenarios. In Case 3-1, if the initial temperature difference is large (larger than ΔT, which will be defined later), the difference will decrease in the next Δt period (as depicted in Fig. 4(c)); however, in Case 3-2, if the initial temperature difference is small (smaller than ΔT), the difference may be further enlarged in the next Δt period (as depicted in Fig. 4(d)). From Fig. 4(d) in Case 3-2, it can be inferred that, the maximum temperature difference after Δt occurs when the initial temperature of the two bitumen tanks is infinitely close to each other, which is shown in Fig. 4(e). This maximum temperature difference, noted as ΔT, can be calculated as follows:

$$\Delta T = \frac{P_{\text{rate}} - U \times A \times \left(T_{n,h-1} - T_{\text{amb}}^h\right)}{c_v \times m} \times \Delta t + \frac{U \times A \times \left(T_{n,h-1} - T_{\text{amb}}^h\right)}{c_v \times m} \times \Delta t$$
$$= \frac{P_{\text{rate}} \times \Delta t}{c_v \times m}$$

$$(13)$$

The above analysis can prove that *Lemma A* is true. Therefore, for the proposed two-layer control method, as long as the very initial value of δ before the first time step of the scheduling horizon is smaller than ΔT, the temperature of each bitumen tank will not exceed the upper/lower limits ($T_{\text{up/down}}$) at any time step.

4. Artificial neural network-based real-time predictive control

4.1. Uncertainty analysis

It can be seen from (5) that the temperature transfer process of a bitumen tank is affected by various uncertainty factors, including the overall heat transfer coefficient (U-value) of the bitumen tank and ambient temperature.

$$U = \frac{1}{\frac{1}{\alpha_1} + \frac{1}{\alpha_2} + \frac{\sigma_1}{\lambda_1} + \frac{\sigma_2}{\lambda_2} + \frac{\sigma_3}{\lambda_3}}$$

$$(14)$$

where α_1 is the individual convection heat transfer coefficient for bitumen; α_2 is the individual convection heat transfer coefficient for ambient air; σ_1 is the steel wall thickness; λ_1 is the thermal conductivity of the steel; σ_2 is the tin sheet thickness; λ_2 is the thermal conductivity of the tin sheet; σ_3 is the insulation thickness; λ_3 is the thermal conductivity of the insulation.

Eq. (14) shows that the U-value is influenced by multiple factors, such as the convection heat transfer coefficient for bitumen and ambient

air [28]. For example, during the operation, the ambient conditions around a bitumen tank can vary due to weather conditions, air velocity, temperature, and humidity. In windy, rainy, and snowy weather, the convection heat transfer coefficient of ambient air is usually higher due to increased air movement around the bitumen tank [29]. On the other hand, in sunny or calm weather, the convection heat transfer coefficient of ambient air is lower, resulting in slower heat transfer from the bitumen tank to the surrounding air. Moreover, the U-value is also influenced by factors such as thermal conductivity, the specific heat capacity of the tank material, and steel wall thickness [30]. If the properties of the materials used in the construction of the bitumen tanks vary between tanks, then the U-values of each tank will also be different. Therefore, the day-ahead control commands of bitumen tanks may not be executable in real-world scenarios due to the impact of uncertain factors, resulting in poor operational performance.

4.2. Modification of ANN-based output

An ANN-based real-time predictive control method is developed in this subsection to mitigate the negative impact of uncertainties in equipment parameters and environmental factors on the operation of bitumen tanks.

Fig. 5 depicts the schematic diagram of an ANN, which is a model consisting of an input layer, hidden layers, and an output layer [31]. After setting hyperparameters, including the number of layers in the hidden layers and the quantity of neurons, the ANN can be trained with a large amount of input and output data. During the training process, the connection weights and bias terms of the ANN are adjusted to enable the network to adapt to input data and generate the desired outputs. In this study, according to the operation of bitumen tanks under various operating conditions, a lot of input data can be obtained, which can be utilized to obtain the output data through the proposed two-layer control method. Therefore, a substantial amount of data for training the ANN can be obtained. Specifically, the input data for training the ANN includes the current temperature within the bitumen tanks, wind power, infrastructure load, and forecasted ambiance temperature. The output data for training is the total ON number of bitumen tanks at each time slot. Once the ANN has been trained, it can be used in the real-time predictive control process to obtain control commands of bitumen tanks based on the updated inputs.

Due to the output data of the ANN-based method being linear numbers, there is a constraint that the output data should be rounded to integer numbers, representing the total ON numbers of bitumen tanks.

$$x_{\text{ANN}}^h = \text{round}\left(x_{\text{out}}^h\right), \forall h$$
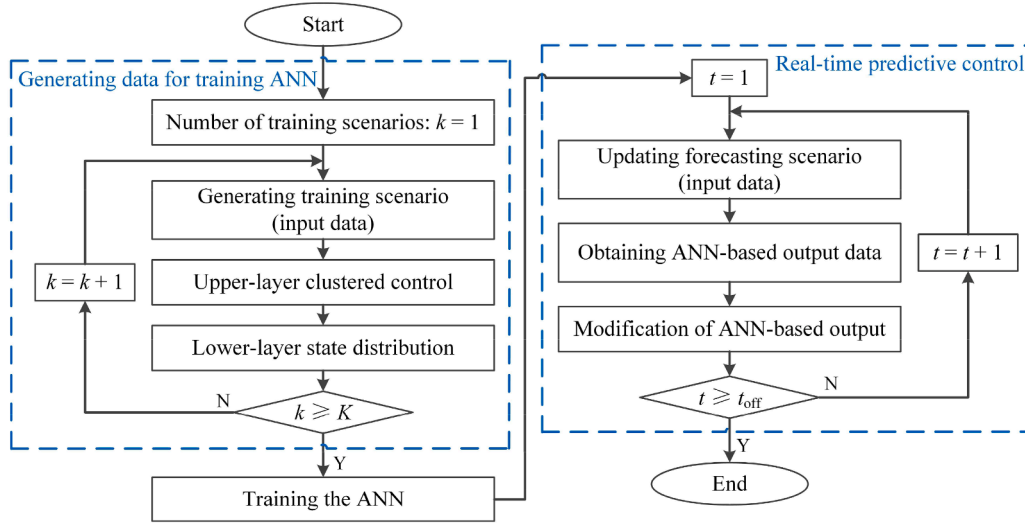
$$(15)$$

Fig. 6. Architecture diagram of the proposed data-driven real-time predictive control method.

where x_{out}^h (linear number) is the output total ON number of bitumen tanks at hth time slot; x_{ANN}^h is the rounded total ON number of bitumen tanks at hth time slot.

Subsequently, the lower-layer state distribution introduced in Section 3-2-2) can also be used to obtain the ANN-based control command of each bitumen tank at each time slot.

It should be noted that, influenced by factors such as network structure, parameter settings, and training data, the output data of ANN may not always be the optimal solution [32]. Therefore, it is necessary to modify the obtained ANN-based control command of each bitumen tank if implementing the command would lead to the violation of the temperature limits during real-time operation.

The mathematical process for the modification is as follows:

$$T_{i,1} = T_{i,0} + \frac{P_{rate} \times x_{ANN}^{i,1} - U \times A \times \left(T_{i,0} - T_{amb}^1\right)}{c_v \times m} \times \Delta t, \forall i \quad (16)$$

$$x_{ANN}^{i,1\,'} = \begin{cases} x_{ANN}^{i,1}, & \text{if } T_{down} \leq T_{i,1} \leq T_{up} \\ 1 - x_{ANN}^{i,1}, & \text{if } T_{i,1} > T_{up} \text{ or } T_{i,1} < T_{down} \end{cases}, \forall i \quad (17)$$

where $x_{ANN}^{i,1}$ is the first control command of the ith bitumen tank based on ANN; $x_{ANN}^{h,1\,'}$ is the modified first control command of ith bitumen tank based on ANN.

Eq. (16) calculates the temperature of each bitumen tank after the execution of $x_{ANN}^{i,1}$. Eq. (17) is given to check whether the temperature of each bitumen tank after executing $x_{ANN}^{i,1}$ violates the upper/lower temperature limits. If the constraint of upper/lower temperature is violated, then the control command obtained from the ANN for the corresponding bitumen tank should be changed.

To facilitate understanding, the architecture diagram of the proposed data-driven real-time predictive control method is exhibited in Fig. 6. In Fig. 6, K is the required number of training scenarios to train the ANN, and t_{off} is the end time of real-time predictive control. Firstly, training data required for the ANN is generated through the two-layer control method. Subsequently, the trained ANN is applied in the solution of real-time predictive control processes for bitumen tanks.

5. Case studies

In this section, several cases are carried out to verify the effectiveness of the two-layer control method of bitumen tanks and the ANN-based real-time predictive control solutions. All cases were performed on a

Table 1
Basic parameters.

Parameter	Value	Parameter	Value	Parameter	Value
N	30	H	96	U (kWm^{-2}K^{-1})	7.75×10^{-3}
A (m^2)	36	c_v (kJkg^{-1}K^{-1})	1.34	m (kg)	21,500
P_{rate} (kW)	120	Δt (s)	900	T_{up} (°C)	180
T_{down} (°C)	150	/		/	/

64-bit PC with a 3.30-GHz CPU and 8-GB RAM. The YALMIP toolbox in MATLAB and CPLEX 12.6 is used to solve the above IP problems. Moreover, the Neural Network Toolbox in MATLAB is used to solve the ANN-based real-time predictive control problem.

The actual measurements of bitumen tanks at the industrial site come from the open data of National Grid and Open Energi [33]. The basic parameters in this study are listed in Table 1.

5.1. Day-ahead direct control results of bitumen tanks

In this subsection, the day-ahead direct control results for different numbers of bitumen tanks are discussed.

Fig. 7(a) illustrates the power consumption curves of the bitumen tanks when the number of tanks is 10, 20, and 30, respectively. It shows that the shapes of power consumption curves are roughly consistent with the shape of wind power after being absorbed by the infrastructure load. This consistency is due to the objective of minimizing the peak-to-valley difference in the demand power curve from the power grid. The demand power curves from the power grid represents wind power subtracted by the infrastructure load and bitumen tanks. Fig. 7(b) indicates that the direct control system works effectively to minimize the peak-to-valley difference of the demand power curve from the power grid, which ensures a more stable and efficient power supply.

The peak-to-valley differences of the electricity exchange curves under different numbers of bitumen tanks and the corresponding calculation times are listed in Table 2. The results show that the peak-to-valley difference is slightly larger when $N = 10$ compared to $N = 20$ and $N = 30$. This is because the regulation capability of bitumen tanks when $N = 10$ is lower compared to a larger number of bitumen tanks. Moreover, it is evident that the calculation time increases significantly as the number of bitumen tanks increases, which is impractical to be implemented in actual operational practice.
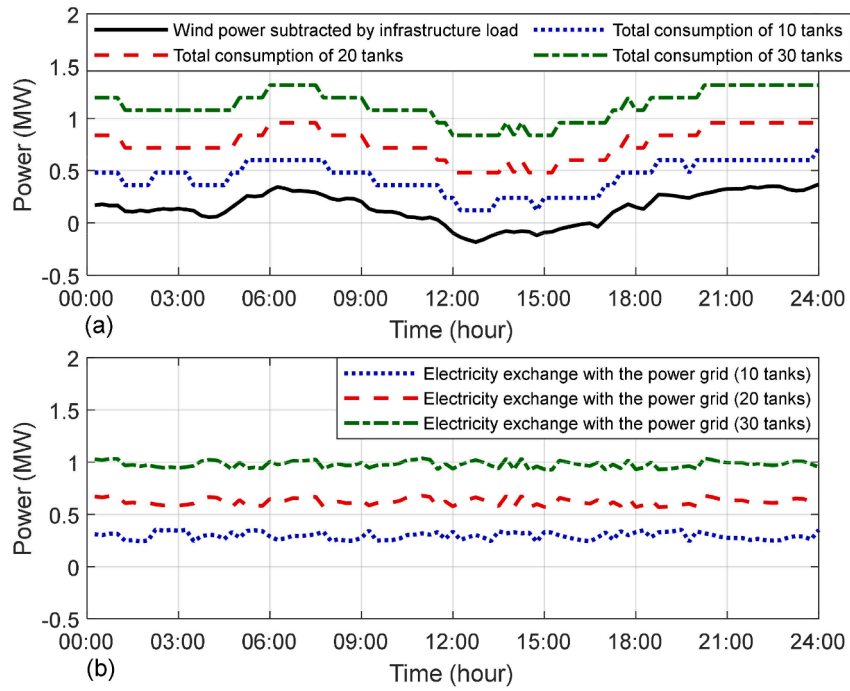
Fig. 7. Day-ahead direct control results for different numbers of bitumen tanks.

Table 2
Day-ahead direct control results under different number of bitumen tanks.

Number of bitumen tanks	Peak-to-valley difference (MW)	Calculation time (s)
10	0.1160	3741.45
20	0.1148	13,873.92
30	0.1148	52,874.13

5.2. Day-ahead two-layer control results of bitumen tanks

In this subsection, the day-ahead two-layer control results of bitumen tanks are discussed. Moreover, the calculation times for day-ahead two-layer control under different control intervals are discussed.

Fig. 8 exhibits the day-ahead two-layer control results with 30 bitumen tanks. It can be observed that the total consumption curve of bitumen tanks in Fig. 8(a) is similar to the day-ahead direct control results, while significantly reducing the calculation time to 41.34 s. Fig. 8 (b) depicts the related temperature transfer process of bitumen tanks, with each colored line representing the temperature variation curve of
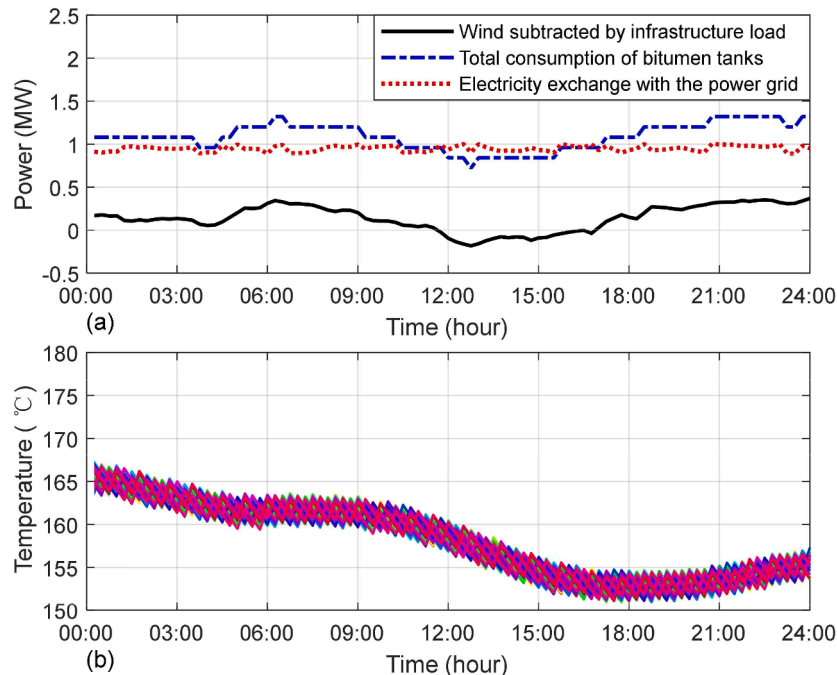

Fig. 8. (a) Day-ahead two-layer control results with 30 bitumen tanks and (b) their temperature transfer process.
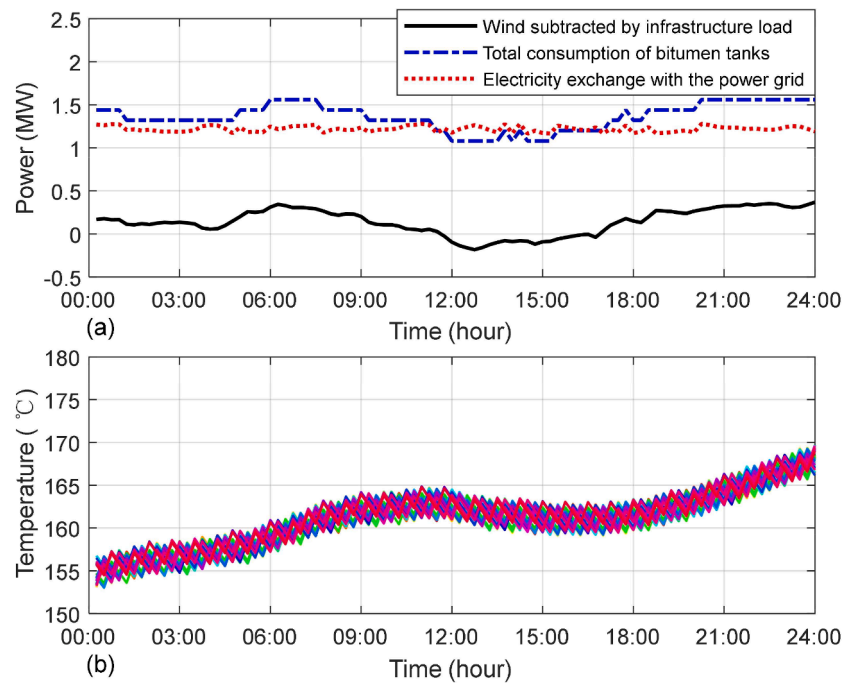
Fig. 9. (a) Day-ahead two-layer control results of 30 bitumen tanks with lower initial heat energy and (b) their temperature transfer process.

Table 3
Day-ahead two-layer control results under different number of bitumen tanks.

Number of bitumen tanks	Peak-to-valley difference (MW)	Calculation time (s)
10	0.1175	41.67
20	0.1193	40.83
30	0.1178	41.34

Table 4
Day-ahead two-layer control results of 30 bitumen tanks under different control interval.

H	Peak-to-valley difference (MW)	Calculation time (s)
96	0.1178	41.34
144	0.1155	104.23
288	0.1142	633.76

an individual bitumen tank. The cluster temperature falls slowly or rises when the total demand power of bitumen tanks is large and drops quickly when it is small. Moreover, Fig. 8(b) shows that there is a temperature loss of about 10° on this day, which means that the initial heat energy in the bitumen tanks will be lower the next day.

To examine the performance of the day-ahead two-layer control method under the condition of lower initial heat energy in the bitumen tanks, the corresponding results are presented in Fig. 9. The lower initial heat energy reduces the downward adjustment space for total consumption of bitumen tanks but increases their upward adjustment space. Therefore, in this situation, the proposed method can still achieve good control performance in terms of the peak-to-valley difference.

To further illustrate the characteristics of the day-ahead two-layer control method, Table 3 presents the calculation times under different number of bitumen tank. A comparison with the data in Table 2 reveals that the calculation time of the two-layer control method is unaffected by the number of bitumen tanks, and there is a significant reduction in calculation time compared to the day-ahead direct control method.

All the above cases are conducted when $H = 96$, with each control interval being 15 min. In Table 4, a comparison of the calculation times for day-ahead two-layer control is provided when the control interval is

shortened to 10 min and 5 min, respectively, while keeping the length of the time horizon unchanged. According to the results presented in Table 4, the calculation time of the two-layer control method increases as the control interval decreases. Meanwhile, with the shortening of the control interval, there is a slight improvement in the peak-to-valley characteristic of the demand power curve.

It is worth noting that in real-time predictive control, for example, with a control interval of 5 min, a calculation time of 633.76 s cannot meet the requirement of real-time operation. Therefore, in this situation, it is necessary to apply the ANN-based method with a faster solving speed.

5.3. Influence of uncertainties

Fig. 10(a) compares the empirical U-value of the bitumen tanks with their potential actual values for a day. The black straight line represents the empirical U-value which remains fixed throughout the day. The colored curves depict the actual variation in U-values for each of the bitumen tanks over time. Fig. 10(b) provides a possible comparison of the forecasted and the actual temperature values of outside ambiance (T_{amb}) during the day, which also affects the temperature transfer process of bitumen tanks.

As claimed in Section 4.1, the actual variation in U-values is influenced by various factors of outside ambiance, including humidity, wind speed, solar radiation, etc. These factors have a high degree of uncertainty, making the accurate forecasting of U-values for each of the bitumen tanks highly challenging. In the predictive control method, the impact of uncertainties in U-values on the temperature transfer of bitumen tanks is considered by updating the real-time temperature of bitumen tanks. This is because the temperature deviation of bitumen tanks, in comparison to day-ahead control, is caused by the impact of various uncertainties. By updating the real-time temperature of bitumen tanks during the predictive control processes, the past impact of uncertainties in U-values can be eliminated. Moreover, unlike the U-values, the forecasting of T_{amb} can be updated with greater accuracy based on data from the local meteorological station during the predictive control processes.

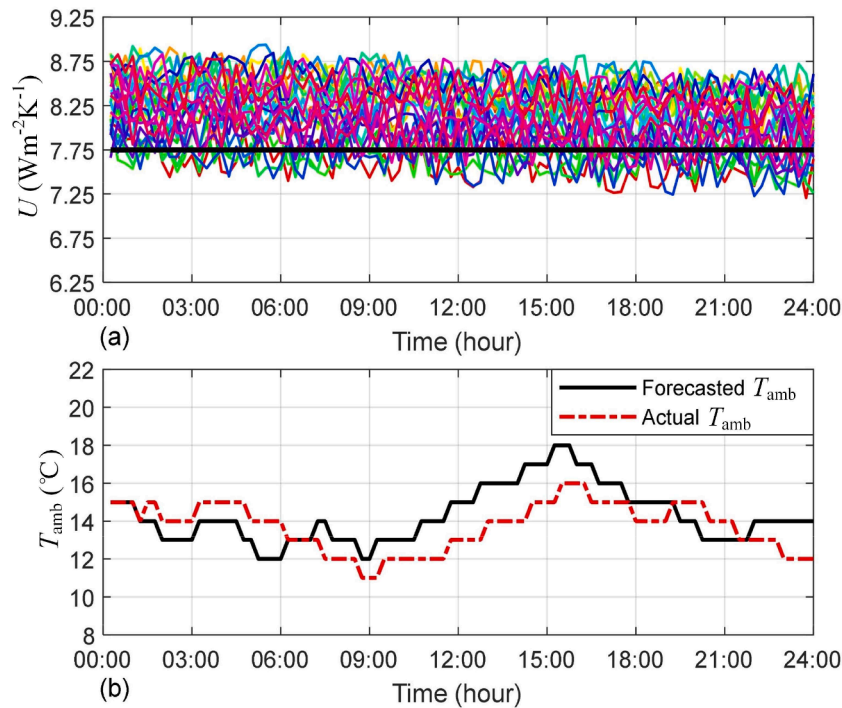Due to the uncertainties and variations in the operation, the actual

Fig. 10. Comparison between (a) the empirical U and (b) the forecasted T_{amb} with their respective actual values.
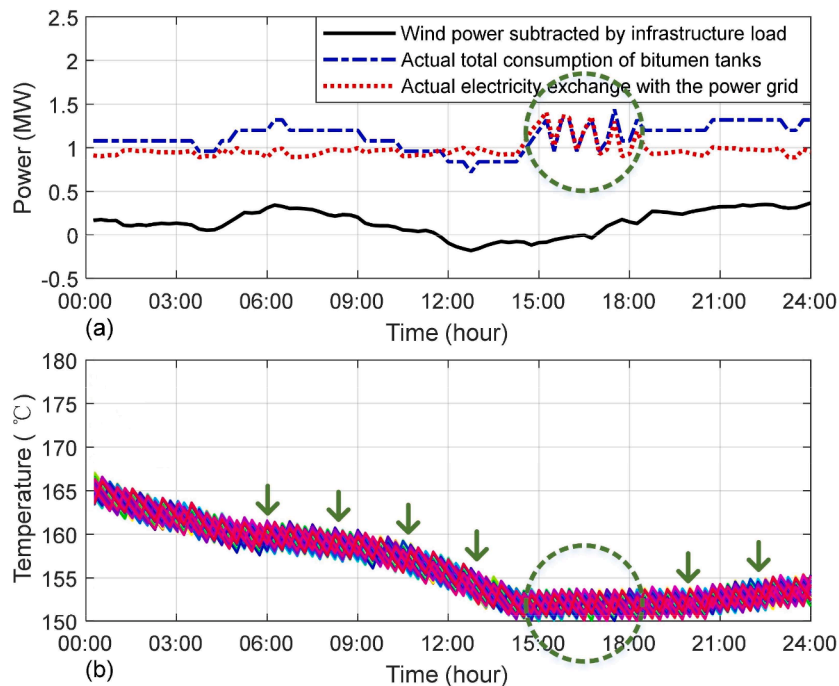

Fig. 11. (a) Actual execution results of day-ahead two-layer control commands with 30 bitumen tanks and (b) their temperature transfer process.

execution of day-ahead two-layer control commands of bitumen tanks may not achieve the desired effects. Fig. 11(a) shows the actual execution results of the day-ahead control commands with 30 bitumen tanks on this day. The overall trend of the total demand power curve is nearly horizontal, with the exception that there are obvious increase and fluctuation during certain periods, as indicated by the circled section in Fig. 11(a), which cause its peak-to-valley difference to increase. Fig. 11 (b) gives the actual temperature transfer process of bitumen tanks.

The reason for the fluctuation in the total demand power curve

within the circled section can be explained as follows. Due to the higher U-values and lower T_{amb}-values in the actual scenario (as shown in Fig. 10), the heat dissipation of bitumen tanks is faster before approximately 14:00, which is illustrated in Fig. 11(b). Therefore, the clustered temperature of bitumen tanks drops rapidly and approaches T_{down} around 14:00. According to the temperature control mechanism, some switches of bitumen tanks are automatically turned ON as their temperatures reach T_{down}. As a result, the day-ahead control commands of switches cannot be executed as planned, leading to increased and

Table 5
Time sequence of switch ON number of bitumen tanks.

Time	15:00	15:15	15:30	15:45	16:00	16:15	16:30
Number	10	11	8	11	11	8	10
Time	16:45	17:00	17:15	17:30	17:45	18:00	18:15
Number	11	8	9	12	9	9	11

Table 6
Training performance of the ANN with different hyperparameters.

N_l	N_n	Regression R value		MSE
		Training data	Validation data	
1	10	0.9719	0.9621	0.6649
	20	0.9824	0.9729	0.4150
	30	0.9915	0.9884	0.2235
	40	0.9937	0.9792	0.3106
	50	0.9951	0.9592	0.5341
2	5	0.9818	0.9670	0.4927
	8	0.9891	0.9780	0.3069
	10	0.9931	0.9817	0.2486
	15	0.9946	0.9613	0.4252
	20	0.9957	0.9428	0.6118

fluctuating power consumption of bitumen tanks during the circled periods.

To explain the reason for the fluctuation in the total demand power curve within the circled section, the time sequence of the switch ON number of bitumen tanks is provided in Table 5. It can be observed that the switch ON number of bitumen tanks changes continuously between 15:00 and 18:00. The reason is that the temperature distribution in bitumen tanks is uneven, causing a varying number of bitumen tanks to automatically switch ON as their temperatures decrease and reach T_{down} at different time stages.

5.4. ANN-based real-time predictive control results

When employing ANN for real-time predictive control, conducting sensitivity analysis on the network hyperparameters is essential to ensure that the trained ANN exhibits good generalization performance. In this study, $K = 1000$ sets of input and output data are generated using the two-layer control model. Among these sets, 80 % are used as training data to train the ANN, while the remaining 20 % are allocated as validation data to assess the generalization performance of the trained ANN.

In Table 6, N_l is the number of hidden layers in the trained ANN; N_n is the number of neurons in each hidden layer. The regression R value is the correlation between the outputs and targets. An R value of 1 indicates a close relationship, while 0 means a random relationship. The mean squared error (MSE) is the average squared difference between the outputs and targets of the validation data, with lower values indicating better accuracy. The results show that when N_l and N_n are relatively small, the regression R value for the validation data increases as N_l and N_n increase. However, if N_l and N_n are too large, it leads to a decrease in the regression R value for the validation data, indicating overfitting. Moreover, DNNs typically have more than 3 hidden layers, making overfitting more likely to occur. Therefore, ANN is more suitable for this study. In Table 6, when $N_l = 1$ and $N_n = 30$, the regression R value and the MSE for the validation data show the best values. Therefore, for the hyperparameters in the ANN, the number of hidden layers is set to 1, with 30 neurons in the hidden layer.

Fig. 12 presents the real-time predictive control results of the ANN-based control commands with 30 bitumen tanks and their temperature transfer process. By continuously utilizing the updated feedback of bitumen tanks, the real-time predictive control method can identify trends indicating that the clustered temperature of bitumen tanks is dropping faster than expected. Therefore, the ANN-based real-time control commands choose to activate more switches during the operation to prevent the cluster temperature from dropping so rapidly. As a result, no switch of bitumen tanks is automatically turned ON in the real-time predictive control process, so the actual total demand power characteristics of the industrial site can be significantly improved. In addition, the average calculation time of obtaining the ANN-based control commands is 0.08 s, which meets the computing time requirement of real-time predictive control.

Fig. 13 compares the electricity exchange curves with the power grid using different control methods of bitumen tanks. Moreover, Table 7 provides a mathematical comparison of different curves in terms of their
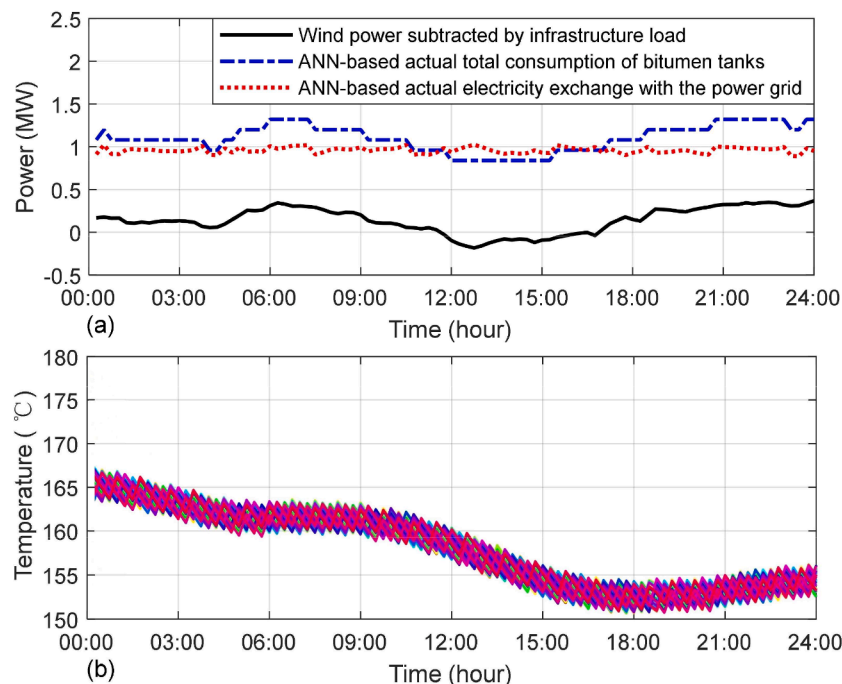

Fig. 12. (a) Real-time predictive control results of ANN-based control commands with 30 bitumen tanks and (b) their temperature transfer process.
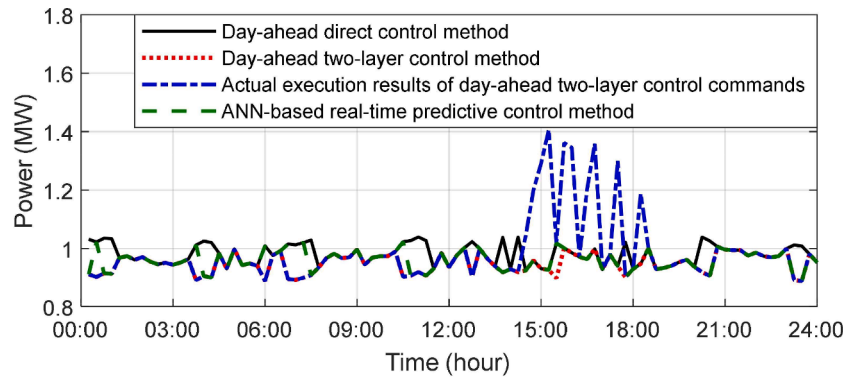
Fig. 13. Comparison of electricity exchange curves with the power grid under different control methods.

Table 7
Comparison of different control methods.

Methods	Peak-to-valley differences (MW)	Time (s)
Day-ahead direct control method	0.1148	28,329.72
Day-ahead two-layer control method	0.1178	41.34
Actual execution of day-ahead method	0.5180	/
ANN-based real-time method	0.1286	0.08

peak-to-valley differences and the calculation times required to obtain the control commands. The peak-to-valley differences of the demand power curves of the day-ahead two-layer control method are nearly the same as that of the day-ahead direct control method, while the calculation times are greatly improved, which indicates the effectiveness of the proposed two-layer control methods. Moreover, compared to the actual execution results of the day-ahead two-layer control commands, the proposed ANN-based predictive control method significantly reduces the peak-valley differences using an extremely short computation time, demonstrating its ability to mitigate the negative impact of uncertainties in the operation of bitumen tanks.

6. Conclusion

To unlock the flexibility potential of industrial heating loads, this paper develops a data-driven real-time predictive control methodology to address the computational complexity and uncertainties in the operational processes of bitumen tanks. Under the computer specifications of a 64-bit PC with a 3.30-GHz CPU and 8-GB RAM, the day-ahead two-layer control method reduces the computation time from 7.87 h to 41.34 s by analyzing and modeling the clustered temperature transfer characteristics of bitumen tanks, enabling the generation of sufficient high-quality data for training ANN. The experimental results of the ANN-based real-time predictive control method demonstrate its effectiveness in managing uncertainties related to equipment parameters and external environmental factors in the industrial operational processes of bitumen tanks. Meanwhile, the ANN-based method can achieve the calculation times as low as 0.08 s, satisfying the computational requirements for the real-time operation of bitumen tanks.

Regarding the applicability, although this paper takes the scheduling of bitumen tanks as a representative to be studied, the proposed approach can be applied to other industrial heating loads, such as industrial aluminum melting pots and industrial steel melting pots. Regarding the limitations, although this study takes into account the uncertainty factors affecting the temperature transfer of bitumen tanks, it overlooks the impact of uncertainties in wind power output and infrastructure load on the control objectives, which should be considered in the future research. Moreover, this paper focuses on a particular

problem, viz., optimal scheduling of bitumen tanks as industrial heat loads. In practical power systems, there will be various types of loads having different characteristics. It will be of more practical significance to consider typical schedulable power system loads along with bitumen tanks to formulate the scheduling problem, which is treated as another future research direction.

CRediT authorship contribution statement

Chuanshen Wu: Writing – original draft, Validation, Software, Data curation, Conceptualization. **Yue Zhou:** Writing – review & editing, Supervision, Methodology. **Jianzhong Wu:** Writing – review & editing, Investigation, Funding acquisition.

Declaration of competing interest

The authors declare that they have no known competing financial interests or personal relationships that could have appeared to influence the work reported in this paper.

Data availability

Information about the data used in the case study of this paper, including how to access them, can be found in the Cardiff University data catalogue at http://doi.org/10.17035/d.2024.0316793297.

References

[1] A. Gholian, H. Mohsenian-Rad, Y. Hua, Optimal industrial load control in smart grid, IEEE Trans. Smart Grid 7 (5) (2015) 2305–2316.
[2] P. Li, W. Sheng, Q. Duan, J. Liang, C. Zhu, A day-ahead peer to peer energy sharing strategy among energy hubs considering flexibility of energy storage and loads, CSEE J. Power Energy Syst. (2022).
[3] C. Huang, H. Zhang, Y. Song, L. Wang, T. Ahmad, X. Luo, Demand response for industrial micro-grid considering photovoltaic power uncertainty and battery operational cost, IEEE Trans. Smart Grid 12 (4) (2021) 3043–3055.
[4] K. Wang, X. Lai, F. Wen, P.P. Singh, S. Mishra, I. Palu, Dynamic network tariffs: current practices, key issues and challenges, Energy Convers. Econ. 4 (1) (2023) 23–35.
[5] M. Kermani, E. Shirdare, A. Najafi, B. Adelmanesh, D.L. Carnì, L. Martirano, Optimal self-scheduling of a real energy hub considering local DG units and demand response under uncertainties, IEEE Trans. Ind. Appl. 57 (4) (2021) 3396–3405.
[6] C. Wu, S. Jiang, S. Gao, Y. Liu, H. Han, Event-triggered model predictive control for dynamic energy management of electric vehicles in microgrids, J. Clean. Prod. 368 (2022) 133175.

[7] S. Yang, M.P. Wan, W. Chen, B.F. Ng, S. Dubey, Model predictive control with adaptive machine-learning-based model for building energy efficiency and comfort optimization, Appl. Energy 271 (2020) 115147.

[8] Z. Zhao, S. Liu, M. Zhou, A. Abusorrah, Dual-objective mixed integer linear program and memetic algorithm for an industrial group scheduling problem, IEEE/ CAA J. Autom. Sin. 8 (6) (2020) 1199–1209.

[9] S. Poikonen, B. Golden, E.A. Wasil, A branch-and-bound approach to the traveling salesman problem with a drone, INFORMS J. Comput. 31 (2) (2019) 335–346.

[10] K. Amine, Multiobjective simulated annealing: principles and algorithm variants, Adv. Oper. Res. 2019 (2019).

[11] C. Wu, H. Han, S. Gao, Y. Liu, Coordinated scheduling for multi-microgrid systems considering mobile energy storage characteristics of electric vehicles, IEEE Trans. Transp. Electrif. (2022).

[12] F. Mumali, Artificial neural network-based decision support systems in manufacturing processes: a systematic literature review, Comput. Ind. Eng. (2022) 107964.

[13] W. Samek, G. Montavon, S. Lapuschkin, C.J. Anders, K.-R. Müller, Explaining deep neural networks and beyond: a review of methods and applications, Proc. IEEE 109 (3) (2021) 247–278.

[14] G. Fragkos, J. Johnson, E.E. Tsiropoulou, Dynamic role-based access control policy for smart grid applications: an offline deep reinforcement learning approach, IEEE Trans. Hum. Mach. Syst. 52 (4) (2022) 761–773.

[15] H. Han, Z. Liu, Y. Hou, J. Qiao, Data-driven multiobjective predictive control for wastewater treatment process, IEEE Trans. Ind. Inform. 16 (4) (2019) 2767–2775.

[16] A. Heuillet, F. Couthouis, N. Díaz-Rodríguez, Explainability in deep reinforcement learning, Knowl. Based Syst. 214 (2021) 106685.

[17] E. Elahi, Z. Zhang, Z. Khalid, H. Xu, Application of an artificial neural network to optimise energy inputs: an energy-and cost-saving strategy for commercial poultry farms, Energy 244 (2022) 123169.

[18] B. Yegnanarayana, Artificial Neural Networks, PHI Learning Pvt. Ltd., 2009.

[19] M. Cheng, J. Wu, S.J. Galsworthy, C.E. Ugalde-Loo, N. Gargov, W.W. Hung, N. Jenkins, Power system frequency response from the control of bitumen tanks, IEEE Trans. Power Syst. 31 (3) (2015) 1769–1778.

[20] A. Olawoyin, Y. Chen, Predicting the future with artificial neural network, Procedia Comput. Sci. 140 (2018) 383–392.

[21] C. Wu, H. Han, S. Gao, Y. Liu, Coordinated scheduling for multimicrogrid systems considering mobile energy storage characteristics of electric vehicles, IEEE Trans. Transp. Electrif. 9 (1) (2022) 1775–1783.

[22] Y. Lin, X. Li, B. Zhai, Q. Yang, J. Zhou, X. Chen, J. Wen, A two-layer frequency control method for large-scale distributed energy storage clusters, Int. J. Electr. Power Energy Syst. 143 (2022) 108465.

[23] M. Castangia, N. Barletta, C. Camarda, S. Quer, E. Macii, E. Patti, Clustering appliance operation modes with unsupervised deep learning techniques, IEEE Trans. Ind. Inform. (2022).

[24] Y. Zhou, M. Cheng, J. Wu, Enhanced frequency response from industrial heating loads for electric power systems, IEEE Trans. Ind. Inform. 15 (6) (2018) 3388–3399.

[25] Y. Zhou, M. Cheng, J. Wu, C. Long, Decentralized control of industrial heating loads for providing multiple levels and types of primary frequency control service, Energy Procedia 158 (2019) 3138–3143.

[26] M. Ghazouani, M. Bouya, M. Benaissa, K. Anoune, M. Ghazi, Thermal energy management optimization of solar thermal energy system based on small parabolic trough collectors for bitumen maintaining on heat process, Solar Energy 211 (2020) 1403–1421.

[27] S. Cai, M. Zhang, Y. Xie, Q. Wu, X. Jin, Z. Xiang, Hybrid stochastic-robust service restoration for wind power penetrated distribution systems considering subsequent random contingencies, IEEE Trans. Smart Grid 13 (4) (2022) 2859–2872.

[28] J. Braziunas and H. Sivilevicius, "Heat transfer and energy loss in bitumen batching system of asphalt mixing plant," in *Environmental Engineering. Proceedings of the International Conference on Environmental Engineering. ICEE*, 2014, vol. 9, p. 1: Vilnius Gediminas Technical University, Department of Construction Economics.

[29] K. Liu, X. Zhang, F. Wang, Y. Da, P. Xu, Thermal transfer analysis method for judging the best time of removing the steel bridge deck asphalt pavement by induction heating, Therm. Sci. Eng. Progr. 37 (2023) 101611.

[30] F. Davie, P. Nolan, T. Hoban, Case histories of incidents in heated bitumen storage tanks, J. Loss Prev. Process Ind. 7 (3) (1994) 217–221.

[31] Y. Sun, S. Li, B. Lin, X. Fu, M. Ramezani, I. Jaithwa, Artificial neural network for control and grid integration of residential solar photovoltaic systems, IEEE Trans. Sustain. Energy 8 (4) (2017) 1484–1495.

[32] W. Bai, Q. Zhou, T. Li, H. Li, Adaptive reinforcement learning neural network control for uncertain nonlinear system with input saturation, IEEE Trans. Cybern. 50 (8) (2019) 3433–3443.

[33] 'Bitumen tanks and systems, 2021'. [Online]. Available: https://www.kvm.dk/wp-content/uploads/2021/05/KVM-International-BITUMEN-EN.pdf.